5 Measurements using the two-layer thin film gauges

5.1 Introduction

The two-layer gauges use thin-films painted on a thin polyamide sheet, which is bonded on the blade surface thanks to a thin adhesive sheet. The latter provides a faster and more flexible implementation than the ceramic inserts. Notice that the last method requires a multi-layer data processing technique, as well as a specific calibration of the thermal properties for each layer (see paragraph 3.9).

The main purpose of the next paragraphs is to validate the results of the two-layer gauges by comparing them with the single-layer gauges, which is a technique that is already used and validated for several times in the VKI CT3 I.L.P. facility.

5.2 Time-averaged component of the two-layer gauges

5.2.1 Initial temperature and Nusselt number calculations

The initial temperature distribution of four tests (52-55) of two-layer gauges (11 gauges used) along the blade is compared with five tests (47-51) of single-layer gauges (18 gauges used) in Figure 5-1. On the graph, the values that correspond to the leading edge area of the blade (L.E.) are represented at the middle, the values of the pressure side (P.S.) on the left and the values of the suction side (S.S.) on the right. The shape of the temperature distribution is similar for both measurement techniques. It is only a lack of chance that the two-layer gauge 513, which looks to suffer more from the windage flow (see paragraph 4.5.2) is missing in this analysis. In Figure 5-2, the two average initial temperature distributions for single and two-layer gauges, shifted at the level of the first experiment, are directly compared on the same graph.

In Figure 5-3, the averaged values of the blade wall temperature during the blowdown (area between the points P_5 and P_6 in Figure 4-3), the corresponding wall heat fluxes and Nusselt numbers are given, for four tests of 11 two-layer gauges. The same analysis is used for the single-layer gauges and it is shown in Figure 4-7. The higher temperatures achieved during the test for the two-layer gauges around the stagnation area of the blade compared to the single-layer ones are evident. This effect is the result of the higher surface insulation of the substrate of the two-layer gauges in comparison to the single-layer ones: the thermal product of Upilex (*692* $J/(m^2Ks^{0.5})$) is much lower than the one of Macor (*1780* $J/(m^2Ks^{0.5})$), which means that the Upilex material resists more to the heat flux penetration. On the other hand, the Nusselt number does not depend on the gauge material but on the flow conditions and the gauge position, both parameters similar for every test. Because of the higher blade wall temperature T_W on the two-layer model compared to the single-layer model during the blowdown, the wall heat flux Q_W of the former is expected to be lower, so that the Nusselt number is similar for both gauges at the same location (Eq. (30)). In reality, for the two-layer gauge that is situated at the stagnation region, gauge 511, the level of its wall heat flux is even higher than the one of the single-layer 211. As a result, the Nusselt number of gauge 511 is 50% higher than the one of gauge 211. The reason can be the high curvature of the blade at the stagnation region, together with the small thickness of the Upilex insulator. Thus, an analysis that takes into account the curvature effects at the leading edge of the blade is of great importance, before a definite conclusion is drawn about the high difference between the Nusselt numbers obtained from gauge 211 and gauge 511. This point is mainly discussed in paragraph 6.2.

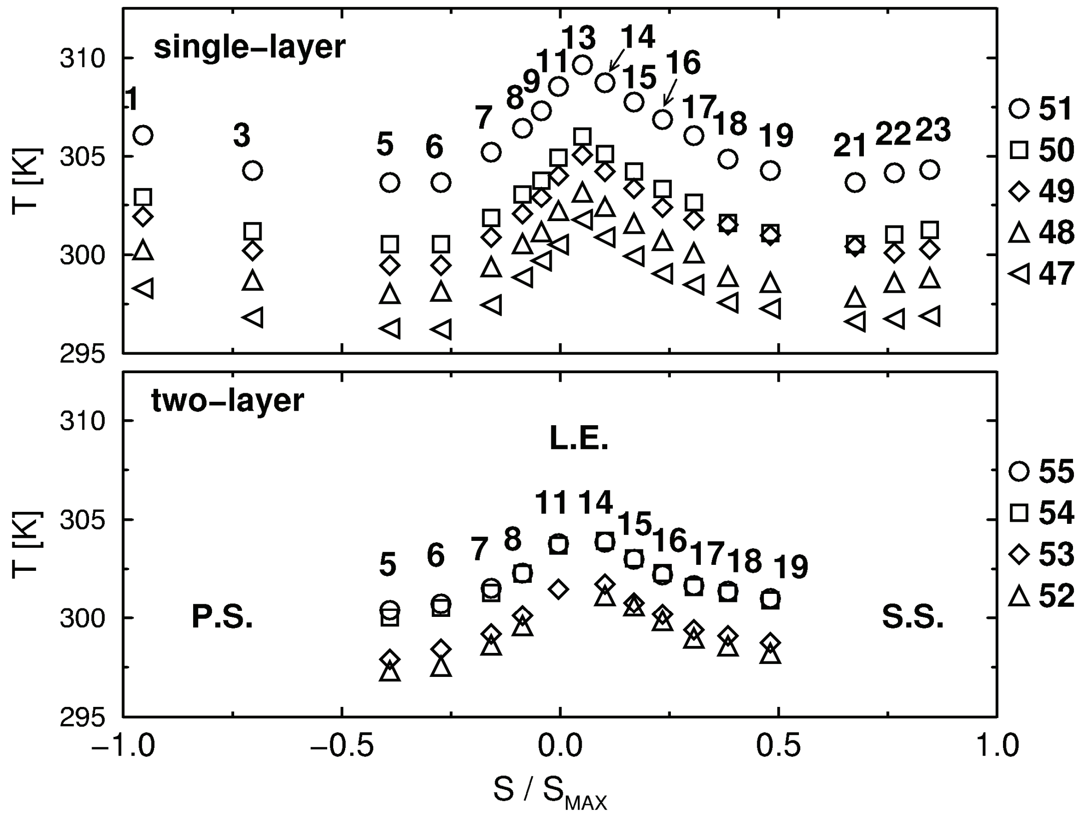

Figure 5-1: Comparison of the initial temperature distribution at 50% span between single and two-layer gauges

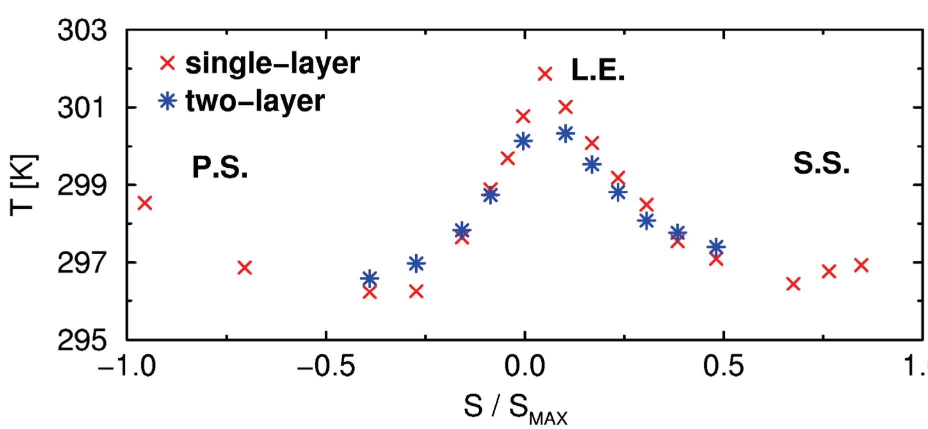

Figure 5-2: The two average initial temperature distributions shifted at the level of the first experiment

In Figure 5-4, the repeatability of the Nusselt number of the two-layer gauges is compared with the repeatability of the single-layer model. It is calculated on the basis of 4 tests on 10 gauges for the two-layer model (40 values) and 5 tests on 17 single-layer gauges, (85 values). The repeatability on the Nusselt number is found equal to ±*55* for the two-layer and ±*103* for the single layer model. The gauges 210 till 212 and 511 give very high differences from test to test, and this is the reason why these gauges are not used for the calculation of the uncertainties. The value of the Nusselt number repeatability depends on the repeatability of the flow conditions during the blowdown.

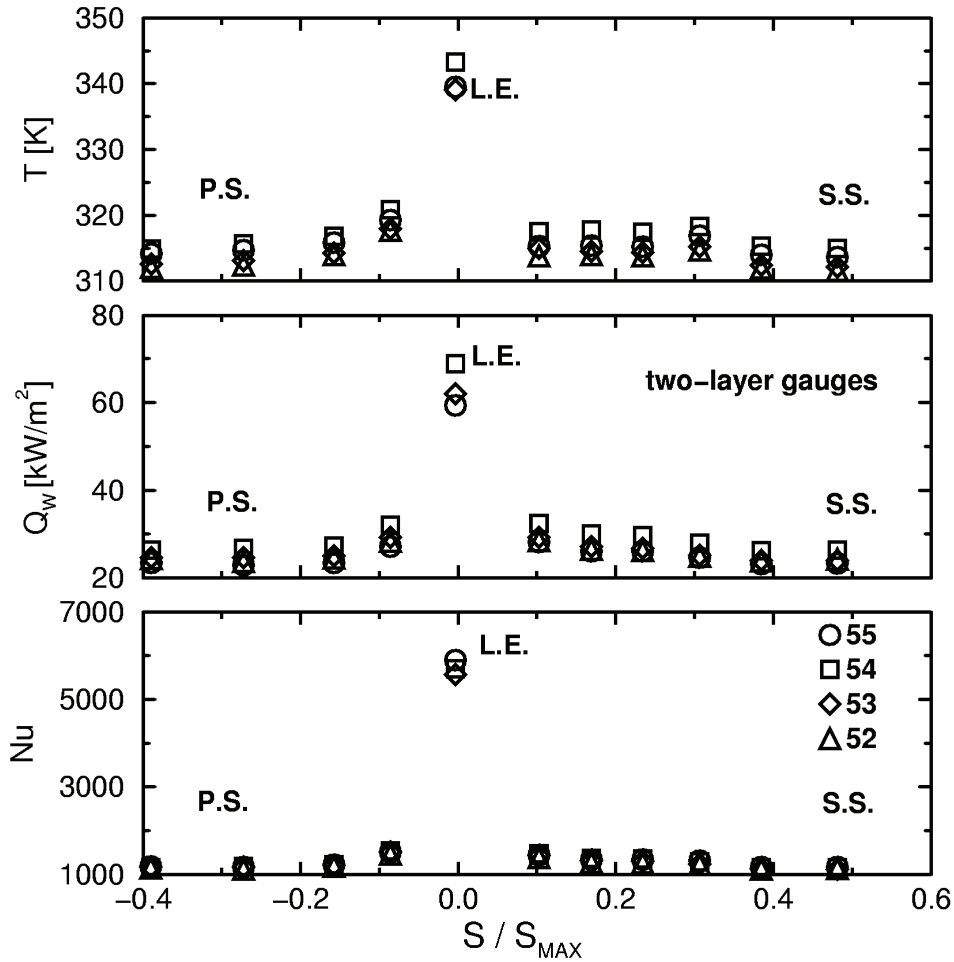

Figure 5-3: Nusselt number distribution at 50% span for the two-layer gauges during the blowdown

For the Nusselt number calculations, it is important to have not only an accurate value of the blade wall temperature (Figure 4-7, Figure 5-3), but also an accurate value of the gas temperature. In our case, measurements have been performed upstream and downstream the second stator. A traverse of 4 thermocouples measures the absolute temperature downstream the rotor, T_{03}, from test number 32 till 48 (see Table 18-2, in Appendix 18.3). One reference thermocouple measures the absolute temperature behind the second stator, T_{04}, from test number 32 till 55. The above analysis has been performed by using as gas temperature, T_{GAS} (Eq. (30)), the value T_{04} multiplied by a factor *1.04*, value that has been calculated as an average ratio of T_{03}/T_{04} for all the measurements performed. In case of an estimation of *10 K* less on the real T_{GAS} value, assuming that the calculation of the blade wall temperature is accurate, an overestimation of the Nusselt number of the order of *150* is generated for the gauge 201. This is equivalent to *+12%* on its average Nusselt number value, an uncertainty whose source is only the uncertainty on T_{GAS}. Because the gas temperature is a reference temperature for the Nusselt number calculations, together with the blade wall temperature, it is suggested that for the next series of tests the T_{03} is also measured at a specific position in front of the stator. Note that although the repeatability of the gas temperature from test to test reaches *14 K*, the blade wall temperature and the wall heat flux values are such, that the repeatability of the final Nusselt number calculations remains in the limits given in Figure 5-4.

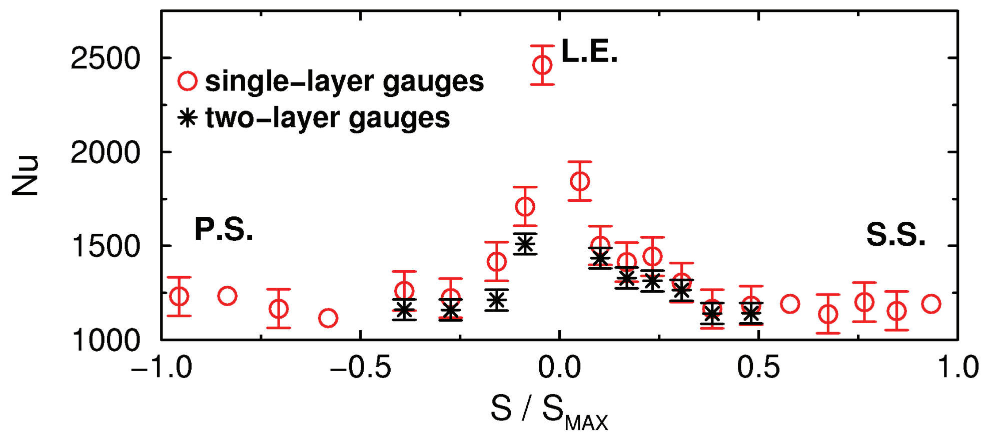

Figure 5-4: Comparison of the repeatability of the Nusselt number distribution at 50% span between single and two-layer gauges

5.3 Time-resolved component of the two-layer gauges

In order to assess the repeatability of the measurements, the Nusselt number traces of two gauges (517 and 506) of four different measurements are given in Figure 5-5. The repeatability of the two-layer gauges seems to be as good as the one of the single-layer model (Figure 4-10).

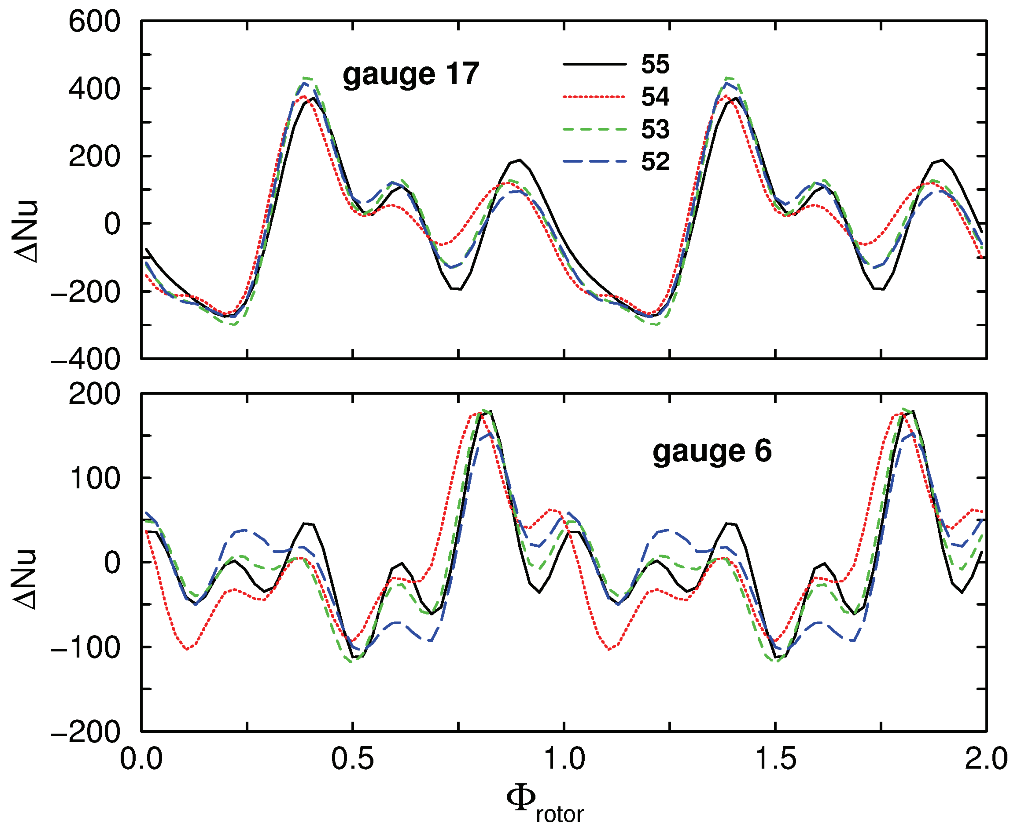

Figure 5-5: Nusselt number traces of two gauges of four different measurements for the two-layer gauges

The minimum-maximum envelope of the phase locked average (*min-max Nu*), the mean *RMS* and the correlation coefficient at 50% span of the two-layer gauges are plotted in Figure 5-6 for a representative test. As far as the *min-max Nu* is concerned, the differences between the single-layer and two-layer gauges do not seem to be significant, although it seems that the correlation coefficient is a bit higher for the two-layer gauges. The former is supposed to be a result of a better resolution (higher signal to noise ratio) on the two-layer gauges in comparison to the single-layer ones and not because of a difference in flow field or in the principles of the measurement technique.

The next step is the comparison of the unsteady Nusselt number traces between the two-layer and the single-layer gauges in Figure 5-7. The results of the two-layer gauges are plotted on top of the single-layer ones indicated by a thinner continuous red line. In general, the maximum and minimum amplitudes of all the Nusselt number traces of the two-layer gauges are at the same rotor phase with the corresponding Nusselt number traces of the single-layer ones. The highest differences are observed for gauges 5, 6, 7 and 8, where the unsteady phenomena of the flow are dominant in that region of the second stator vane.

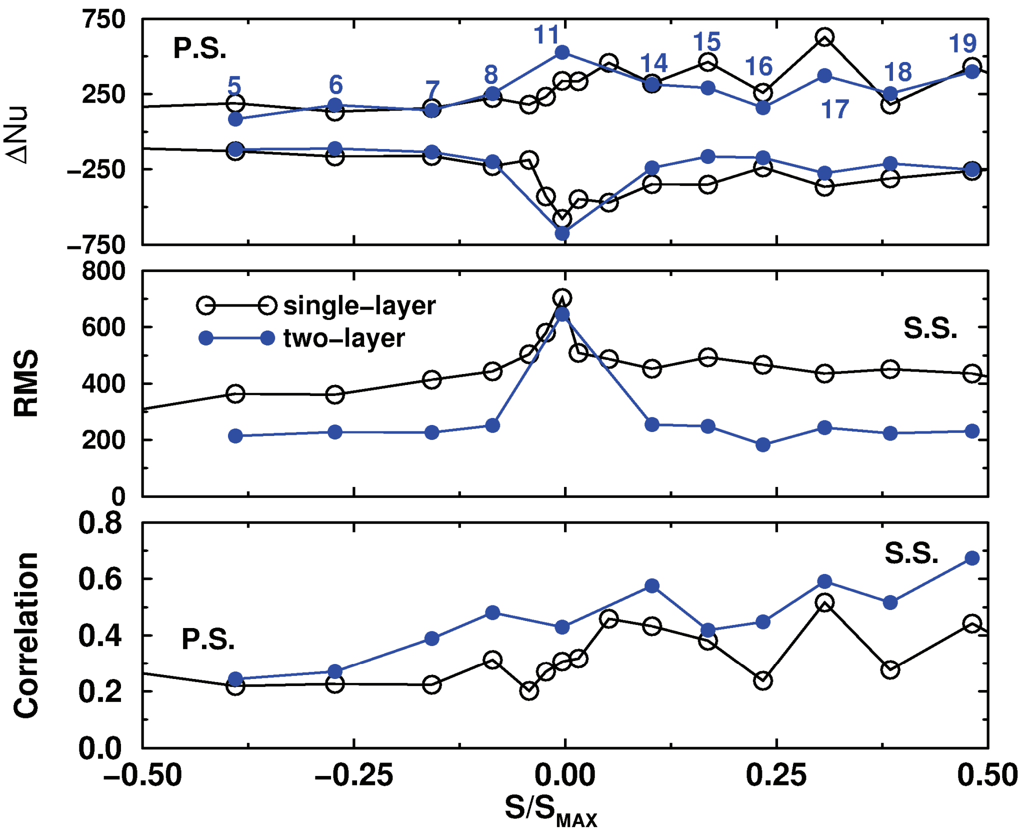

Figure 5-6: Comparison of the statistics for unsteady Nusselt number at 50% span between single and two-layer gauges

Although the comparison of all the Nusselt number traces between the two-layer and the corresponding single-layer gauges is shown in Figure 5-7, the quality of the comparison is considerably enhanced when the scale is higher. The Nusselt number traces for the same gauges 17 and 6 are plotted on the same scale for the two different measurement techniques in Figure 5-8. The traces on the gauge 17 are much closer than the traces of the gauge 6, for the same reasons that were mentioned in paragraph 4.6.2. Note that for the gauge 506, although the amplitude of the Nusselt number is not very close to the one of gauge 206, the local minima and maxima follow the same relative time to the phase of the rotor.

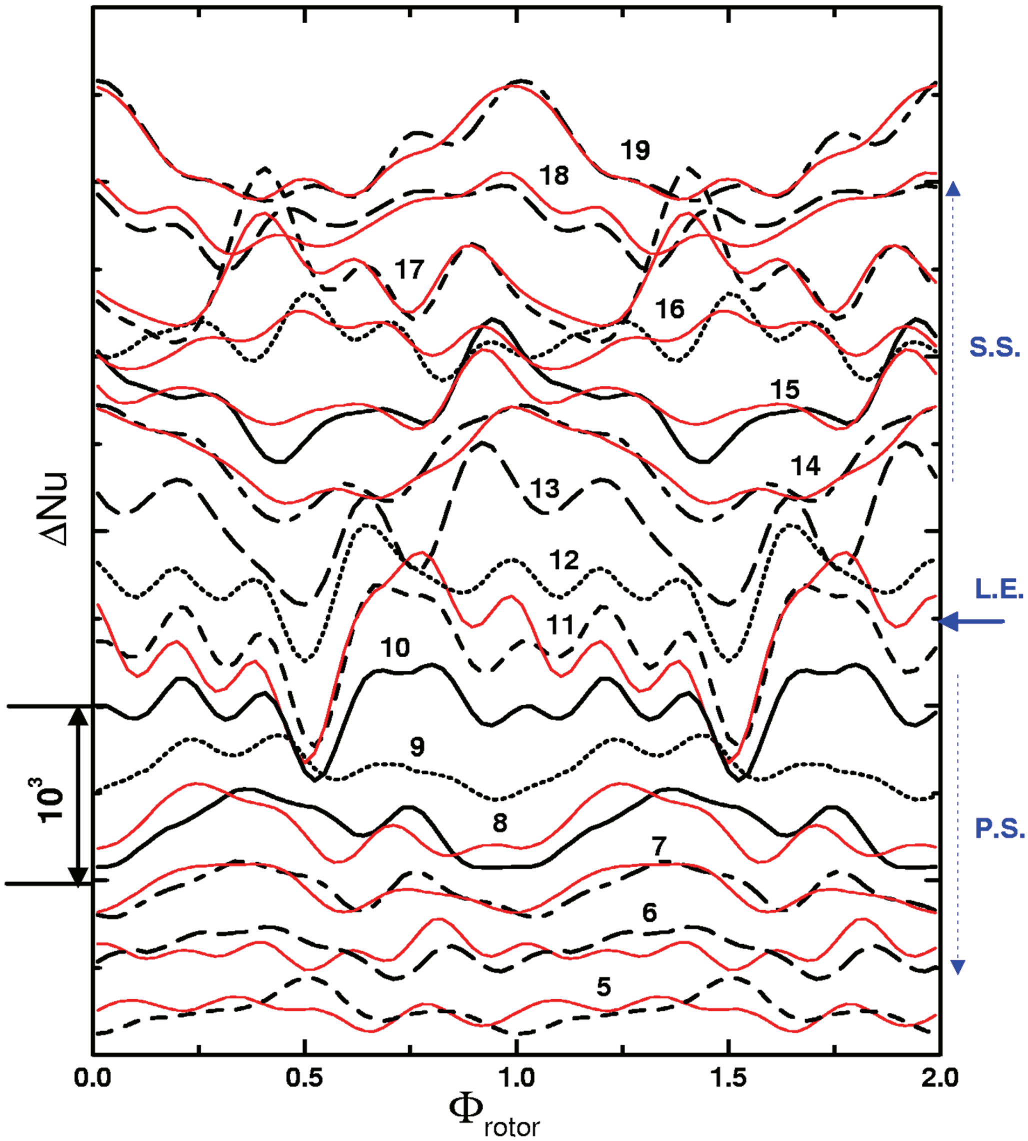

Figure 5-7: Comparison of the unsteady Nusselt number traces between the two-layer and the single-layer gauges

The results from the measurements with the two-layer gauges on the second stator of the CT3 facility are also published by Iliopoulou et al. (2004).

5.4 Conclusions

The environment in which the two-layer gauges are tested in the above analysis, in order to be compared with the single-layer ones, is one of the most difficult, because there are no real dominant phenomena in the flow, except the flow perturbations described in paragraph 4.6.2, whose strength is much lower than in the case of the transonic rotor blades (steady shocks). However, the results of the two measurement techniques are matching in a satisfactory level. The next validation of two-layer gauge technique has to be carried out on rotor blades, where on one hand the fluctuations of the Nusselt number traces will be higher, so easier to be captured by the gauges, but on the other hand the rotor blades will be much more curved than the second stator vanes. The latter introduces additional difficulties on the installation of the gauges on the blades.

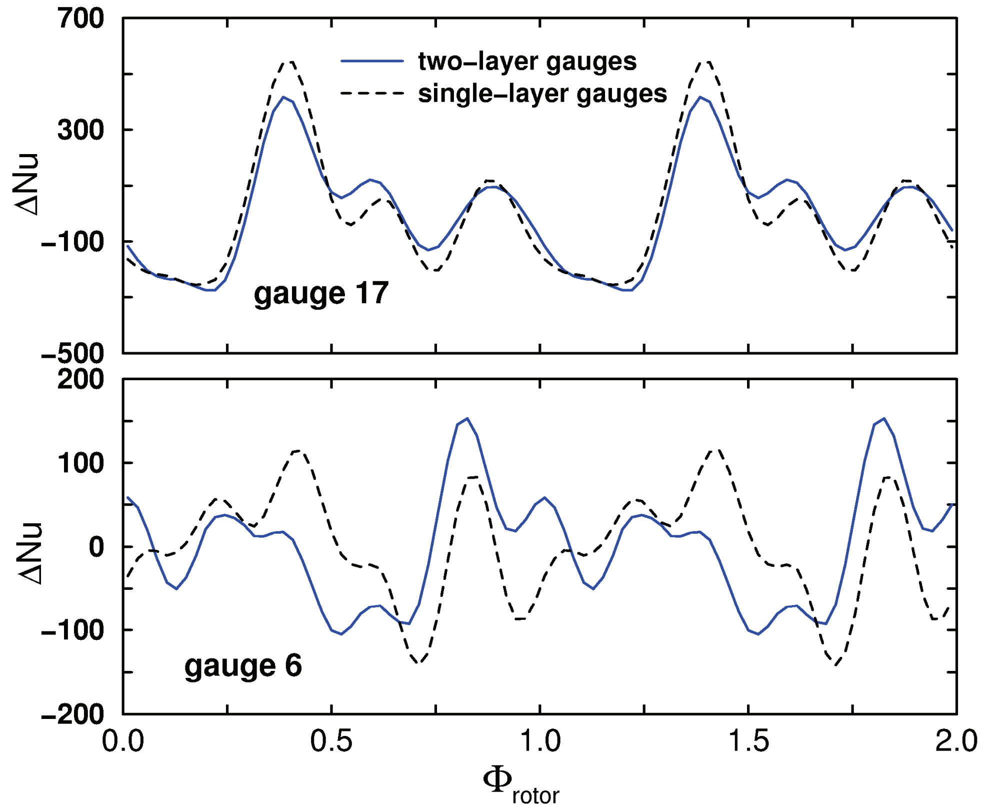

Figure 5-8: Comparison of Nusselt number traces of two gauges for two different measurement techniques

5.5 References

Arts T., Lambert de Rouvroit M., and Rutherford A.W., 1990, ‘*Aero-thermal investigation of a highly loaded transonic linear turbine guide vane cascade - A test case for inviscid and viscous flow computations’*, VKI TN 174

Didier, F., Denos, R. and Arts T., 2002, *‘Unsteady Rotor Heat Transfer in a Transonic Turbine Stage’*, J. of Turbomachinery, vol. 124, no 4, pp 614-622.

Iliopoulou V., Denos R., Billiard N., Arts T., 2004, *‘Time averaged and time-resolved heat flux measurements on a turbine stator blade using two-layered thin-film gauges’*, ASME 2004-GT-53437, Vienna, Austria – J. of Turbomachinery, vol. 126, pp 570-577